Available online at www.sciencedirect.com
SCIENCE DIRECT®
Journal of Sound and Vibration 281 (2005) 189–217
JOURNAL OF SOUND AND VIBRATION
www.elsevier.com/locate/jsvi

Quantification of damping mechanisms of active constrained layer treatments

H. Illaire*, W. Kropp

Department of Applied Acoustics, Chalmers University of Technology, 41296 Göteborg, Sweden

Received 20 January 2003; accepted 12 January 2004
Available online 29 September 2004

Abstract

In active constrained layer (ACL) treatments, a layer of viscoelastic material is bonded to the host structure and constrained by an actuator. Since several mechanisms simultaneously damp vibrations in ACL treatments, quantifying these mechanisms is essential to understand and optimise these treatments. Several approaches in the literature quantify ACL damping mechanisms. However, these approaches do not take into account the reduction of input power into the structure that can be induced by the actuator, although it is known that this reduction is an important mechanism in treatments based on active control.

This paper proposes an approach that allows quantification of all the damping mechanisms of ACL treatments. In this approach, three indices quantify the efficiency of the three identified damping mechanisms: the shearing of the viscoelastic layer in open loop, the increase of shearing in the viscoelastic layer due to the motion of the actuator, and the decrease of total input power into the structure due to the forces applied by the actuator through the viscoelastic layer. The sum of these two last indices quantifies the efficiency of the active actions, and the sum of all three indices quantifies the total efficiency of the ACL treatment.

In order to implement the approach, a wave approach model of beams treated with ACL is selected from the literature and is experimentally validated. The model is used to find numerically the control voltage optimising the efficiency of the active action, and to calculate the resulting quantification indices for the six first modes of partially or fully treated beam. Results indicate that with a high shear modulus of the viscoelastic material, the optimum control voltage is lower and less sensitive to changes of the stiffness that might occur with temperature variations. A high shear modulus also leads to a better complementarity

*Corresponding author. Tel.: +46-31-772-2205; fax: +46-31-772-2212.
E-mail address: helene@ta.chalmers.se (H. Illaire).

0022-460X/$ - see front matter
doi:10.1016/j.jsv.2004.01.032

between the active and passive frequency of the ACL treatment, resulting in a broader effective frequency range. The effect of the forces applied to the structure is to minimise the total input power rather than to maximise the absorption of power by the actuator, suggesting that control laws ensuring absorption of energy by the actuator (and thus the stability of the control) might be suboptimal in terms of vibration reduction. It can be concluded that the quantification indices presented in this work are a powerful tool to get insight into the damping mechanisms of ACL.

1. Introduction

Active constrained layer (ACL) treatments have been extensively investigated during the last decade. Several configurations of ACL have been proposed. The fundamental principle of these designs is to reduce vibrational energy simultaneously by dissipation when shearing a constrained viscoelastic layer, and by the action of an actuator. In the typical configuration shown in Fig. 1, the viscoelastic layer is sandwiched between the structure and the actuator. If the actuator is properly driven, it increases the shearing of the viscoelastic layer and thus the dissipation of energy. In the following, this mechanism will be referred to as ''material damping''. The actuator also applies forces to the host structure, further controlling the vibration. This combination of active control and material damping is the advantage of ACL treatments, because active control is easier to implement at low frequencies, while viscoelastic materials are more efficient at high frequencies. In addition, the presence of material damping adds stability to the system, so that the efficiency of the active control can be improved.

As explained above, the different damping mechanisms simultaneously reduce vibrations in ACL treatments. To be able to optimise these treatments, it is necessary to understand their physical behaviour, and to quantify the different mechanisms involved in the damping process.

An attempt in this direction has been made by Liao and Wang [1], who investigated the influence of viscoelastic material properties on the performance of the ACL treatment. They used a finite-element formulation, together with the Golla–Hughes–McTavish method [2,3], to derive a time-domain model for a beam treated with ACL and excited with broadband noise. In Liao's paper, cost functions associated with the vibration suppression ability and control effort were used to derive three indices. The first one represents the efficiency of the treatment in open-loop configuration, i.e. when no control voltage is sent to the actuator. The second index quantifies the effect of the viscoelastic layer on the force transmission between the actuator and the structure. It is based on the comparison between the ability of the actuator supplied with a DC voltage to

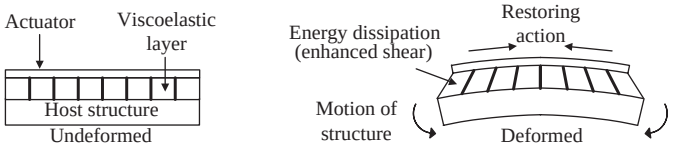

Fig. 1. Principle of active constrained layer.

deflect the beam, in the presence and in the absence of the viscoelastic layer. The third index represents the efficiency of the treatment in closed-loop configuration, i.e. when the active control system is switched on. To derive it, the closed-loop vibration suppression ability is compared with the open-loop vibration suppression ability when the damping of the viscoelastic layer is set to zero, and the difference is normalised by the control effort. This approach allowed the authors to map the parameters of the viscoelastic layer for which the ACL treatment outperforms the pure active control treatment (the treatment with the actuator directly bonded to the structure). However, it does not make it possible to quantify each mechanism separately when the treatment is made active. Therefore the influence of, e.g. the control voltage on each mechanism could not be investigated.

A different approach is based on power considerations. Shen [4] showed that the power input by the external forces applied to a structure treated with ACL, is dissipated simultaneously by the shearing of the viscoelastic layer and by the absorption of energy at the actuator. He proposed, simultaneously as Baz [5] a control law ensuring that energy is dissipated by the actuator and thus guaranteeing stability of the control. In another article, Baz [6] derived an expression quantifying the passive loss factor from the power dissipated in the viscoelastic layer. Similarly, an active loss factor was derived from the power absorbed by the actuator, and the total loss factor of the system was the sum of both. This approach was used by several authors to optimise the design of ACL treatments [7–10].

However, it does not take into account the change of impedance of the structure that can be the result of the actuator action, although it is known that the change of impedance, and thus of input energy from external sources, is an important mechanism of active control [11]. In fact, Brennan et al. [12] showed that on a beam with primary and secondary forces, minimising the total input power (i.e. the input power from both sources) is a better strategy than maximising the energy absorption by the secondary forces. This minimisation cannot be quantified by a loss factor, since the vibration reduction in this case is not due to a dissipation of energy.

In the present work, the efficiency of all the damping mechanisms of ACL is quantified by a set of indices, based on the kinetic energy and the power balance of the structure. Three indices quantify the efficiency of the three identified damping mechanisms: the shearing of the viscoelastic layer in open loop, the increase of shearing in the viscoelastic layer due to the motion of the actuator, and the decrease of total input power into the structure due to the forces applied by the actuator through the viscoelastic layer. The sum of these two last indices quantifies the efficiency of the active actions, and the sum of all three indices quantifies the total efficiency of the ACL treatment. To implement this approach, it is necessary to have a model describing structures treated with ACL. A model based on the wave approach is used to predict the response of beams treated with ACL. It is similar to the one derived by Baz [13,14], besides a few modifications. The beams are resting on springs at their ends, and can be treated with ACL on part or whole of their length. The model is validated experimentally up to 2 kHz. Using the model, two numerical studies are made to illustrate the approach. In the first numerical study, the beam is fully treated and the shear modulus of the viscoelastic layer, supposed to be constant with frequency, is varied. In the second numerical study, the beam is partially treated and is suspended on soft springs at its ends, and actual data is used for the shear modulus of the viscoelastic layer. This numerical study highlights the effect of dissipative boundary conditions and of the frequency dependence of the

shearing of the viscoelastic material, on the performance of the ACL treatment. In both studies, the model is used to find numerically the control voltage optimising the efficiency of the active action, and to calculate the resulting quantification indices for the six first modes of beams treated with ACL. Results show that the quantification indices presented in this work are a powerful tool to get insight into the damping mechanisms of ACL.

The derivation of the model is presented in Section 2, and its validation in Section 3. In Section 4, the indices quantifying the damping mechanisms of ACL treatments are described. A parameter study illustrating the approach on a beam fully treated with ACL is presented in Section 5. In this parameter study, the effect of the shear modulus of the viscoelastic layer on the different quantification indices is investigated. Finally in Section 6, the indices are computed for a beam partially treated with ACL and suspended on soft springs at its ends.

2. Model

Several models of structures treated with ACL have been presented in the literature. The model presented here is based on Baz' work [13,14], and uses a wave approach. The advantage of the wave approach is that there is no need to make assumptions on the shape functions of the structure. The details of the derivations that can be found in Baz' work will not be repeated here; the purpose of this section is to resume Baz' model, as well as to present the modifications made to it.

The model describes the vibrational behaviour of beams fully or partially treated with ACL. Although it might be more interesting to focus on panels with respect to typical industrial applications of ACL, the emphasis of this work is on understanding the physical mechanisms of ACL, and a simple one-dimensional wave guide is well suited for this purpose. For the same reason, no control law is included in the model; instead, the phase and amplitude of the control voltage can be chosen freely so that it is possible to investigate their effect on the different damping mechanisms.

The three-layers system resulting from the assembly of the beam, the viscoelastic layer and the constraining layer, is described in Fig. 2. In the following, the subscript letters b, v and c will refer to the base layer, the viscoelastic layer and the cover layer, respectively.

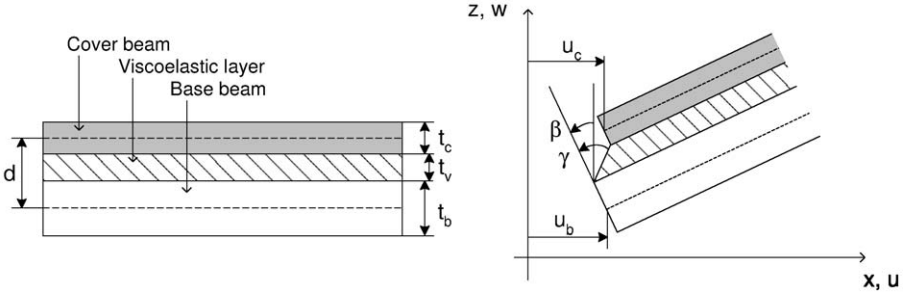

Fig. 2. The three-layers system.

2.1. Assumptions

Several assumptions are made in the model:

- The classical Euler–Bernouilli assumptions apply for the base and cover layers;
- the deflection in normal direction to the surface is the same for all layers, i.e. no compression with respect to the thickness occurs in any of the layers;
- only shear motion is assumed to take place in the viscoelastic layer. The shear angle is constant across the depth of the viscoelastic layer;
- only bending waves are assumed to propagate in the base and cover layers.

2.2. The wave equation

The wave equation of the three-layers system can be obtained either by writing the equilibrium of forces and moments for each layer [13], or by using Hamilton's principle [5,4] (the reader is referred to the literature for the detail of the derivation). The wave equation is given by

$$\frac{\partial^6 w}{\partial x^6} - g(1+Y)\frac{\partial^4 w}{\partial x^4} + \frac{\rho}{D_t}\left(\frac{\partial^2 \ddot{w}}{\partial x^2} - g\ddot{w}\right) = 0, \tag{1}$$

where w is the normal displacement of the structure, and ρ is the density per unit length of the three-layers system. The quantities g, D_t and Y are given by

$$g = \frac{G}{t_v}\left(\frac{1}{E_b t_b} + \frac{1}{E_c t_c}\right), \tag{2}$$

$$D_t = E_b I_b + E_c I_c, \tag{3}$$

$$Y = b\frac{d^2}{D_t}\frac{E_b t_b E_c t_c}{E_b t_b + E_c t_c}, \tag{4}$$

where

- G is the complex shear modulus of the viscoelastic layer, defined by $G = G'(1+\mathrm{i}\eta)$, where G' is the storage modulus and η is the loss factor of the viscoelastic material;
- E_b and E_c are the elasticity moduli of the base and cover layers;
- I_b and I_c are the moments of inertia of the base and cover layers;
- t_b, t_v and t_c are the thicknesses of the layers;
- the width of the beam is b;
- $d = t_v + (t_b + t_c)/2$ is the distance between the neutral lines of the base and cover layers.

An interesting interpretation of the variables D_t, g and Y has been given by Ungar [15] as follows: if k is the wave number of a prescribed bending wave on the beam, it can be shown that g/k^2 is proportional to the ratio of a flexural wavelength to the distance within which a local shear disturbance decays to $1/e$ of its value. Thus, g/k^2 is a measure of how well the viscoelastic layer

couples the flexural motions of the two elastic substructures. Also, one can show that the effective complex flexural rigidity D of the composite structure is given by

$$D = D_t\left(1 + \frac{\chi^*}{1+\chi^*}\, Y\right), \tag{5}$$

where * denotes the complex conjugate, and $\chi = g/k^2$. For $\chi = 0$, the composite flexural rigidity is then equal to the sum of flexural rigidities of the base and cover layers, as if they were unconnected. For large χ, D tends toward $D_t(1 + Y)$, which can be shown to correspond to the flexural rigidity of the composite if the viscoelastic layer has a very large shear stiffness (its Young's modulus still remaining negligible). Thus, one may also interpret the geometric parameter Y as

$$1 + Y = \frac{D_{\chi\to\infty}}{D_{\chi\to 0}} = \frac{D_{\text{coupled}}}{D_{\text{uncoupled}}}. \tag{6}$$

2.3. Wave approach formulation

The solution is assumed to have the form of a wave

$$w(x,t) = W(x)\mathrm{e}^{\mathrm{j}\omega t} = C\mathrm{e}^{\delta x}\mathrm{e}^{\mathrm{j}\omega t}, \tag{7}$$

where δ is the wavenumber and ω is the radian frequency. Inserting this expression into Eq. (1) yields

$$\lambda^6 - g(1+Y)\lambda^4 - \frac{\rho}{D_t}\,\omega^2\lambda^2 + \frac{\rho}{D_t}\,g\omega^2 = 0, \tag{8}$$

where λ is the differential operator with respect to x. This equation has six roots $\pm\delta_1$, $\pm\delta_2$ and $\pm\delta_3$, given by

$$\delta_1^2 = \gamma_1 + \gamma_2 + \frac{g}{3}(1+Y), \tag{9}$$

$$\delta_2^2 = -\frac{\gamma_1+\gamma_2}{2} + \mathrm{j}\,\frac{\sqrt{3}}{2}\,(\gamma_1-\gamma_2) + \frac{g}{3}\,(1+Y), \tag{10}$$

$$\delta_3^2 = -\frac{\gamma_1+\gamma_2}{2} - \mathrm{j}\,\frac{\sqrt{3}}{2}\,(\gamma_1-\gamma_2) + \frac{g}{3}\,(1+Y), \tag{11}$$

where

$$\gamma_1 = \sqrt[3]{-\frac{\xi_2}{2} + \sqrt{\frac{\xi_1^3}{27} + \frac{\xi_2^2}{4}}}, \quad \gamma_2 = \sqrt[3]{-\frac{\xi_2}{2} - \sqrt{\frac{\xi_1^3}{27} + \frac{\xi_2^2}{4}}} \tag{12}$$

and

$$\xi_1 = -\frac{\rho\omega^2}{D_t} - \tfrac{1}{3}g^2(1+Y)^2, \quad \xi_2 = g\,\frac{\rho\omega^2}{D_t} - \tfrac{1}{3}g(1+Y)\,\frac{\rho\omega^2}{D_t} - \frac{2}{27}\,g^3(1+Y)^3. \tag{13}$$

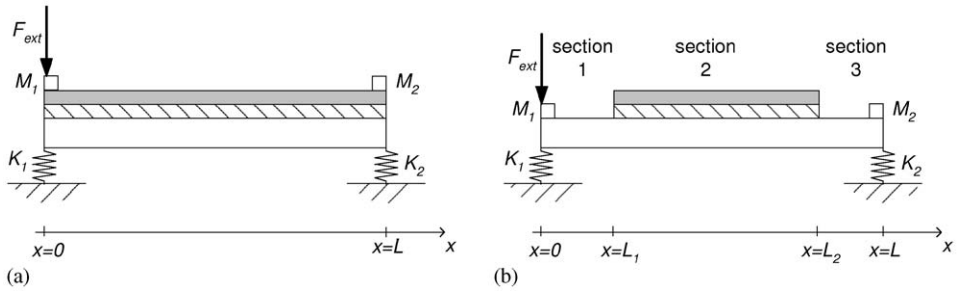

Fig. 3. The modelled structures: (a), fully treated beam; (b), partially treated beam.

Inserting these roots into Eq. (7) leads to

$$W(x) = C_1 e^{\delta_1 x} + C_2 e^{-\delta_1 x} + C_3 e^{\delta_2 x} + C_4 e^{-\delta_2 x} + C_5 e^{\delta_3 x} + C_6 e^{-\delta_3 x}, \tag{14}$$

where the six constants C_1–C_6 are to be determined. To avoid numerical problems on implementation, Eq. (14) is rewritten

$$W(x) = C_1 e^{-\delta_1 (L-x)} + C_2 e^{-\delta_1 x} + C_3 e^{-\delta_2 (L-x)} + C_4 e^{-\delta_2 x} + C_5 e^{-\delta_3 (L-x)} + C_6 e^{-\delta_3 x}, \tag{15}$$

where L is the position of the end of the treatment. In this way, very large values of the exponentials with positive argument are avoided.

2.4. Boundary conditions

In the following, the cases of a fully treated beam and of a partially treated beam are considered (see Fig. 3). In both cases, the beam is resting at its ends on springs of stiffness K_1 and K_2. If the springs are sufficiently soft, the beam can be considered freely suspended above the resonance frequencies of the resulting mass–spring system. The advantage of this configuration over a free–free one, is that the amplitude of the rigid body modes will have a finite amplitude. If a control law is to be implemented, this will remove the problem of having "infinite" amplitudes at very low frequencies. This configuration is also preferred over a cantilever one, because an ideal clamped boundary condition is difficult to realise in practice, while spring mounting is easy to implement.

Mass loading effects are included in the model, so that it is possible to take into account the weight of measuring equipment, represented by two masses M_1 and M_2 at the two ends of the beam.

2.4.1. Fully treated beam

Six equations are needed to find the six unknowns C_1–C_6. These equations are obtained by writing the equilibrium of forces and moments at both ends of the beam.

The moments at the ends of the beam are vanishing

$$M|_{x=0} = M|_{x=L} = 0. \tag{16}$$

In this expression, M is the total moment applying on the cross-section of the three-layers system and is given by[1]

$$M = -\frac{D_t}{g}\left(\frac{\partial^4 W}{\partial x^4} - (Y+1)g\,\frac{\partial^2 W}{\partial x^2} - \frac{\rho\omega^2}{D_t}\,W - Y\,\frac{g}{d}\,\varepsilon_p\right). \tag{17}$$

In this equation, ε_p is the free strain induced in the active constraining layer by the control voltage V_c, and is given by

$$\varepsilon_p = \frac{d_{31}}{t_c}\,V_c, \tag{18}$$

where d_{31} is the strain constant of the piezoelectric material.

Longitudinal forces are vanishing at both ends of the beam and thus

$$\left.\frac{\partial U_b}{\partial x}\right|_{x=0} = \left.\frac{\partial U_b}{\partial x}\right|_{x=L} = 0. \tag{19}$$

In this equation, U_b is defined by

$$u_b(x,t) = U_b(x)\mathrm{e}^{\mathrm{j}\omega t}, \tag{20}$$

where u_b is the longitudinal displacement of the neutral line of the base beam (see Fig. 2). The derivative of U_b is given by

$$\frac{\partial U_b}{\partial x} = -\frac{D_t}{K_b b d}\left(\frac{1}{g}\,\frac{\partial^4 W}{\partial x^4} - Y\,\frac{\partial^2 W}{\partial x^2} - \frac{\rho\omega^2}{D_t g}\,W - \frac{Y}{d}\,\varepsilon_p\right). \tag{21}$$

At the position $x = L$, the transversal force V applied to the cross-section of the three-layers system is the sum of the force F_{K_2} applied by the spring and of the force F_{M_2} applied by the mass of measuring equipment:

$$V|_{x=L} = F_{K_2} + F_{M_2}, \tag{22}$$

where

$$V = -\frac{D_t}{g}\left(\frac{\partial^5 W}{\partial x^5} - g(1+Y)\,\frac{\partial^3 W}{\partial x^3} - \frac{\rho\omega^2}{D_t}\,\frac{\partial W}{\partial x}\right), \tag{23}$$

$$F_{K_2} = -K_2 W(L), \tag{24}$$

$$F_{M_2} = M_2\,\omega^2 W(L). \tag{25}$$

At $x = 0$, the external force F_{ext} also has to be taken into account

$$-V|_{x=0} = F_{K_1} + F_{M_1} + F_{\mathrm{ext}}, \tag{26}$$

with

$$F_{K_1} = -K_1 W(0), \tag{27}$$

[1]The reader is referred to Ref. [13] for the derivation of the equation above.

and

$$F_{M_1} = M_1 \omega^2 W(0). \tag{28}$$

In Eq. (26), the transversal force V is written with a minus sign. This is because forces and moments, by convention, are taken on the right-hand side of elements of the beam. But at $x = 0$, it is the force applied to the left-hand side of the element that has to be taken into account.

Inserting Eq. (15) into the six equations given in Eqs. (16), (19), (22) and (26), leads to the following matrix equation:

$$\begin{bmatrix} A_1 e^{-\delta_1 L} & A_1 & A_2 e^{-\delta_2 L} & A_2 & A_3 e^{-\delta_3 L} & A_3 \\ Q_1 e^{-\delta_1 L} & Q_1 & Q_2 e^{-\delta_2 L} & Q_2 & Q_3 e^{-\delta_3 L} & Q_3 \\ R_1 e^{-\delta_1 L} & R_1 & R_2 e^{-\delta_2 L} & R_2 & R_3 e^{-\delta_3 L} & R_3 \\ B_1 & B_1 e^{-\delta_1 L} & B_2 & B_2 e^{-\delta_2 L} & B_3 & B_3 e^{-\delta_3 L} \\ Q_1 & Q_1 e^{-\delta_1 L} & Q_2 & Q_2 e^{-\delta_2 L} & Q_3 & Q_3 e^{-\delta_3 L} \\ R_1 & R_1 e^{-\delta_1 L} & R_2 & R_2 e^{-\delta_2 L} & R_3 & R_3 e^{-\delta_3 L} \end{bmatrix} \begin{pmatrix} C_1 \\ C_2 \\ C_3 \\ C_4 \\ C_5 \\ C_6 \end{pmatrix} = \begin{pmatrix} F_{\text{ext}} \\ -\frac{btE_b E_c d_{31}}{E_b t_b + E_c t_c} V_c \\ \frac{D_t Y}{d} \frac{d_{31}}{t_c} V_c \\ 0 \\ -\frac{btE_b E_c d_{31}}{E_b t_b + E_c t_c} V_c \\ \frac{D_t Y}{d} \frac{d_{31}}{t_c} V_c \end{pmatrix}. \tag{29}$$

In this expression

$$A_i = -(-n)^2 P_i + M_1 \omega^2 - K_1, \quad i = 1, 2, 3, \tag{30}$$

$$B_i = -(-n)^2 P_i - (M_2 \omega^2 - K_2), \quad i = 1, 2, 3, \tag{31}$$

where n is the number of the column in which A_i and B_i appear. Also,

$$P_i = \frac{D_t}{g}\left(\delta_i^5 - g(1 + Y)\delta_i^3 - \delta_i \frac{\rho\omega^2}{D_t}\right), \tag{32}$$

$$Q_i = -\frac{D_t}{dg}\left(\delta_i^4 - gY\delta_i^2 - \frac{\rho\omega^2}{D_t}\right), \tag{33}$$

$$R_i = \frac{D_t}{g}\left(\delta_i^4 - g(1 + Y)\delta_i^2 - \frac{\rho\omega^2}{D_t}\right), \tag{34}$$

where i takes the values 1,2,3.

Note that all terms containing the control voltage V_c have been passed to the right-hand side of Eq. (48). In this way, the control voltage sent to the actuator is considered as an external excitation and can be chosen to be any value.

2.4.2. Partially treated beam

As described in Fig. 3, the beam is now treated with ACL between the positions $x = L_1$ and L_2. The treated portion of the beam is referred to as section 2, while the bare portions are referred to as sections 1 and 3. In the following, the subscript numbers 1, 2, and 3 will refer to the different sections of the beam.

As a difference from Baz' model [14], the longitudinal waves in sections 1 and 3 of the beam are not considered, and only bending motion is assumed to take place in these sections. This is consistant with the assumption that only bending waves are propagating in the base and cover layers of the three-layers system. Such an assumption is realistic because longitudinal waves generally occur at frequencies much higher than those of bending waves. Accordingly, sections 1 and 3 of the beam are described with Euler–Bernouilli's theory. The transversal displacement in these sections is assumed to have the form

$$w_{1,3}(x,t) = W_{1,3}(x)\mathrm{e}^{\mathrm{j}\omega t} = C\mathrm{e}^{-kx}\mathrm{e}^{\mathrm{j}\omega t} \tag{35}$$

and obeys

$$W_1(x) = C_7\mathrm{e}^{-k(L_1-x)} + C_8\mathrm{e}^{-kx} + C_9\mathrm{e}^{\mathrm{j}kx} + C_{10}\mathrm{e}^{-\mathrm{j}kx} \tag{36}$$

in section 1 of the beam, and

$$W_3(x) = C_{11}\mathrm{e}^{-k(L-x)} + C_{12}\mathrm{e}^{-kx} + C_{13}\mathrm{e}^{\mathrm{j}kx} + C_{14}\mathrm{e}^{-\mathrm{j}kx} \tag{37}$$

in section 3 of the beam. In Eqs. (36) and (37), the wavenumber of bending waves is $k = \sqrt[4]{\rho_b\omega^2/E_bI_b}$ (ρ_b is the density of the base beam). The transversal displacement W_2 in section 2 of the beam obeys Eq. (15), as in the case of the fully treated beam.

Fourteen boundary and continuity conditions are necessary to solve the unknowns C_1–C_{14}.

In sections 1 and 3 of the beam, the transversal forces V_1 and V_3 at the ends of the beam obey

$$V_1|_{x=0} = -F_{K_1} - F_{M_1} - F_{\mathrm{ext}}, \tag{38}$$

$$V_3|_{x=L} = F_{K_2} + F_{M_2}, \tag{39}$$

where

$$V_i = -E_bI_b\frac{\partial^3 W_i}{\partial x^3}, \quad i = 1,3 \tag{40}$$

and F_{K_1}, F_{K_2}, F_{M_1} and F_{M_2} are the same as in Eqs. (24)–(25) and (27)–(28). The moments M_1 and M_3 obey

$$M_1|_{x=0} = M_3|_{x=L} = 0, \tag{41}$$

where

$$M_i = E_bI_b\frac{\partial^2 W_i}{\partial x^2}, \quad i = 1,3. \tag{42}$$

The boundary conditions at $x = 0$ and L result in four equations, therefore ten equations at the positions $x = L_1$ and L_2 are necessary. Eight of them are given by the continuity of the variables corresponding to bending motion, i.e. the continuity of deflection,

$$W_1|_{x=L_1} = W_2|_{x=L_1}, \quad W_2|_{x=L_2} = W_3|_{x=L_2}, \tag{43}$$

bending angle,

$$\left.\frac{\partial W_1}{\partial x}\right|_{x=L_1} = \left.\frac{\partial W_2}{\partial x}\right|_{x=L_1}, \quad \left.\frac{\partial W_2}{\partial x}\right|_{x=L_2} = \left.\frac{\partial W_3}{\partial x}\right|_{x=L_2}, \tag{44}$$

transversal forces,

$$V_1|_{x=L_1} = V_2|_{x=L_1}, \quad V_2|_{x=L_2} = V_3|_{x=L_2}, \tag{45}$$

and moments,

$$M_1|_{x=L_1} = M_2|_{x=L_1}, \quad M_2|_{x=L_2} = M_3|_{x=L_2}, \tag{46}$$

have to be fulfilled. In the expressions above, the moment M_2 and the transversal force V_2 in the treated section are the same as M and V in Eqs. (17) and (23).

The boundary conditions given by Eqs. (43)–(46) are different to those given by Baz [14], where boundary conditions are given by the continuity of derivatives of W until the fourth order. However, assuming the continuity of forces and moments is a more physical approach. Note that at the junctions $x = L_1$ and L_2, the moments and forces in sections 1 and 3 have to be equalised with the moments and forces applied to the whole cross-section of the treated part. This is because the three-layers system is treated as a single layer with equivalent properties.

The two last equations are given by the boundary conditions applied to the cover beam. At $x = L_1$ and L_2, the stresses in the longitudinal direction vanish

$$\left.\frac{\partial U_c}{\partial x}\right|_{x=L_1} = 0, \quad \left.\frac{\partial U_c}{\partial x}\right|_{x=L_2} = 0. \tag{47}$$

The 14 boundary conditions given in Eqs. (38)–(41), (43)–(46) and (47), together with Eqs. (15), (36) and (37), lead to the following matrix equation:

$$\mathbf{AC} = \mathbf{F}, \tag{48}$$

where $\mathbf{C}$ is a vector containing the 14 unknowns C_1–C_{14}, and $\mathbf{A}$ and $\mathbf{F}$ are given in the appendix.

2.5. Derivation of the field variables

Once all the wave amplitudes C_1–C_{14} have been derived, the deflection of the beam can be obtained using Eqs. (15) and (36)–(37). The other field variables can be derived by using the equations resulting from the equilibrium of forces and moments on the three-layers construction. Among the important field variables are the shear strain γ, given by

$$\gamma = \frac{D_t}{Gbdg}\left(\frac{\partial^5 W}{\partial x^5} - gY\frac{\partial^3 W}{\partial x^3} - \frac{\rho\omega^2}{D_t}\frac{\partial W}{\partial x}\right), \tag{49}$$

and the longitudinal displacement of the base beam U_b given by

$$U_b = -\frac{D_t}{E_b t_b bdg^2}\left(\frac{\partial^5 W}{\partial x^5} - gY\frac{\partial^3 W}{\partial x^3} - \left(\frac{\rho\omega^2}{D_t} + Yg^2\right)\frac{\partial W}{\partial x} - \frac{g^2 Y}{d}\varepsilon_p x\right). \tag{50}$$

3. Experimental validation

The models for fully and for partially treated beams were experimentally validated. The experiments were made in steps of increasing complexity: first on untreated beams, then on beams treated with passive constrained layer (PCL) and finally on beams treated with ACL. In each experiment, the driving point mobility was measured at one end of the beam. In all the experiments, the properties of the base beam, described in Table 1, were the same, and the beam was resting on springs at its ends. These springs were made of a piece of foam (Sylomer S80) and their stiffness K_1 and K_2 were determined from the measurements.

3.1. Untreated beam

The goal of measuring an untreated beam was to check the quality and limitations of the experimental setup. The measured driving point mobility was compared with the predictions given by the model presented in Section 2. The results are shown in Fig. 4. The agreement between model and measurement is excellent up to 2 kHz. The experimental setup can therefore be used successfully over a large frequency range. The beam suspended on springs results in a mass–spring

Table 1
Base beam properties

Material	Length	Width	Thickness	Young's modulus	Density
Aluminium	0.4 m	0.03 m	2.92×10^{-3} m	69×10^{9} N/m^2	2680 kg/m^3

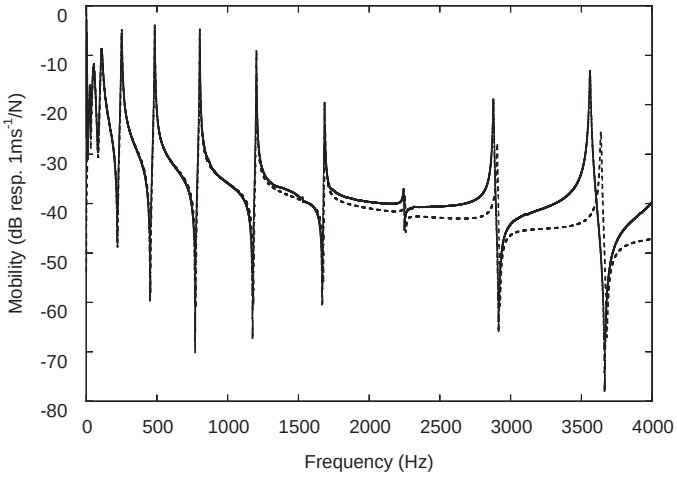

Fig. 4. Driving point mobility of the untreated beam: ——, measured; - - -, calculated.

system, whose resonance frequencies are made visible in Fig. 5. The driving point mobility calculated for the free–free case is also plotted. This shows that the effect of the springs on the first bending modes is not negligible, although the stiffness of the springs was chosen as low as possible.

3.2. Beam with PCL treatment

In the case of beams fully or partially treated with PCL, the treatment was realised with a damping tape manufactured by 3M (#2552). It was made of a layer of viscoelastic material and of a layer of aluminium, whose properties are given in Table 2. The complex shear modulus G of the viscoelastic material is a function of both frequency and temperature. The data for G was provided by J. Rongong, who extracted it from the normograph given by 3M, and is shown in Fig. 6 for a temperature of 20°C. As shown in Figs. 7 and 8, the agreement between measurements and theoretical predictions is excellent, both in the case of fully and of partially treated beams.

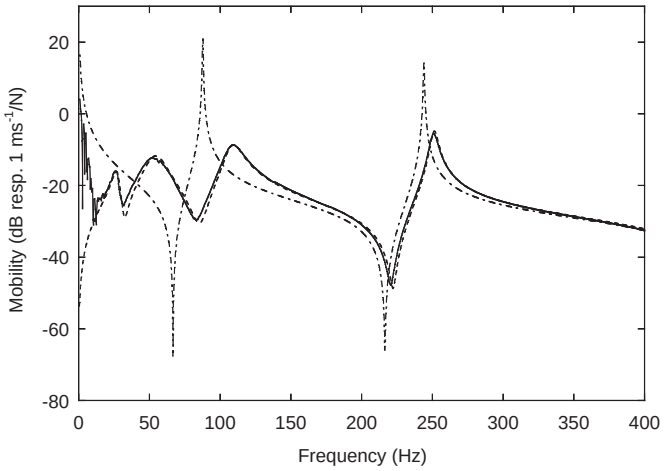

Fig. 5. Driving point mobility of the untreated beam (zoom at low frequencies): ——, measured; - - -, calculated; - · -, calculated with $K_1 = K_2 = 0$.

Table 2
PCL treatment properties

Material	Width	Thickness	Young's modulus	Density
Aluminium	0.03 m	0.254×10^{-3} m	69×10^{9} N/m^2	2700 kg/m^3
3M ISD 112	0.03 m	0.127×10^{-3} m	See Fig. 6	1130 kg/m^3

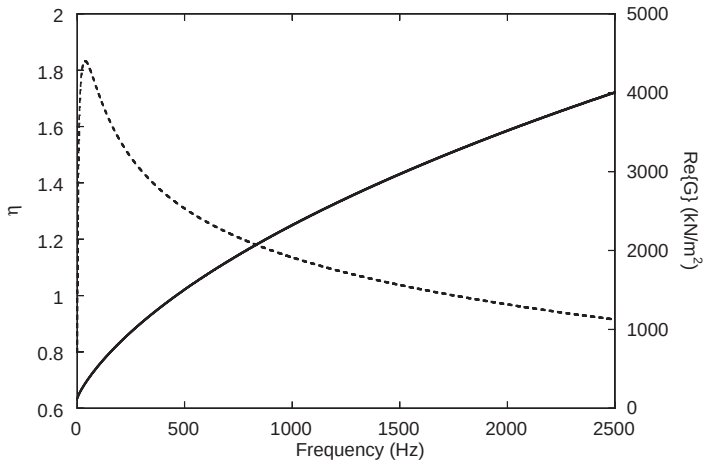

Fig. 6. Shear modulus and loss factor of viscoelastic material 3M ISD112: - - -, η; ——, Re{G}.

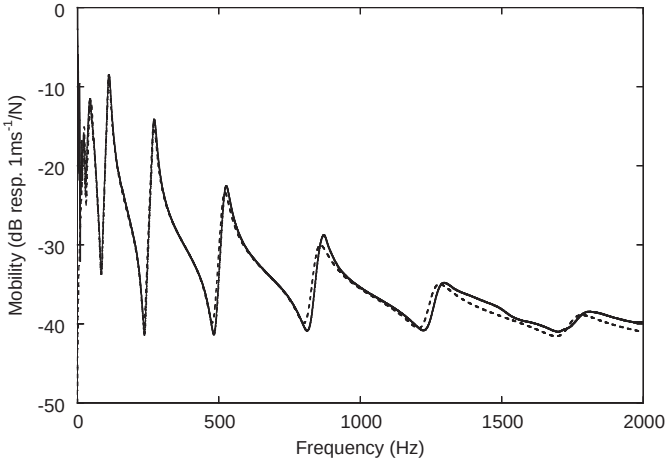

Fig. 7. Driving point mobility of the fully treated beam: ——, measured; - - -, calculated.

3.3. Beam with ACL treatment

The experiments were only made on a beam partially treated with ACL, because of the limited size of available piezoceramic plates. The constraining layer was made of an actuator (PIC 255, manufactured by PI) whose properties are given in Table 3. A layer of viscoelastic material was sandwiched between the actuator and the base beam; it was made of the same material as the one used in PCL treatments, see Table 2. The ACL patch was positioned slightly off-centre on the beam, starting at $x = 0.198$ m.

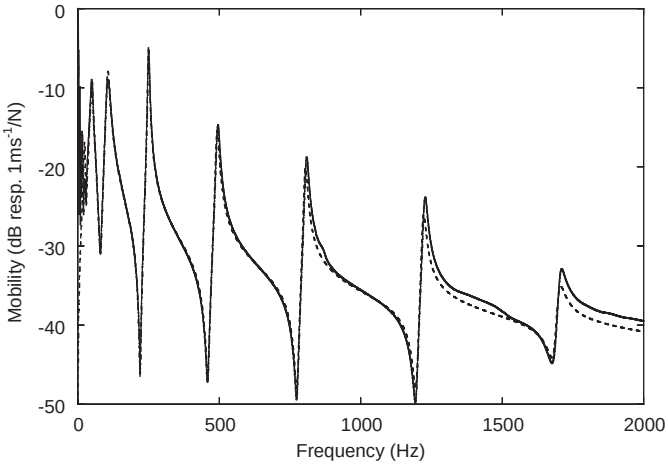

Fig. 8. Driving point mobility of the partially treated beam ($L_1 = 0.15\,\text{m}$, $L_2 = 0.25\,\text{m}$): ——, measured; - - -, calculated.

Table 3
Actuator properties

Material	Length	Width	Thickness	Young's modulus	Density	d_{31}
PZT	0.05 m	0.03 m	5×10^{-4} m	62.1×10^{9} N/m^2	7800 kg/m^3	-18×10^{-13} m/V

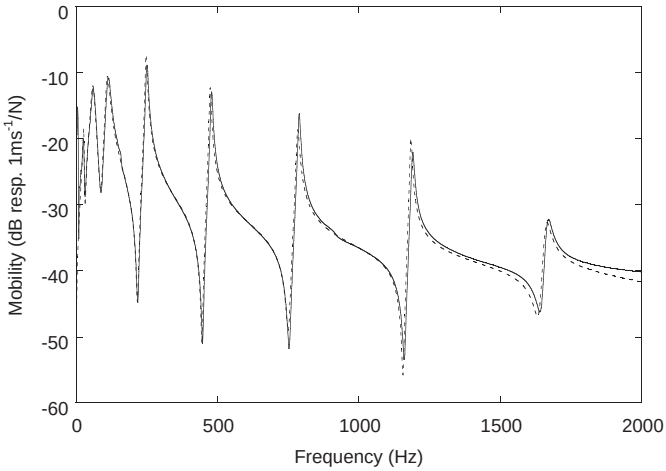

Fig. 9. Mobility of a beam treated with ACL and excited with a shaker: ——, measured; - - -, calculated.

The validation of the model in the case of an ACL treatment makes use of the linearity of the system under consideration. The driving point mobility of the beam, when only a point force is applied to one of its ends, is presented in Fig. 9. The response of the beam at the same point when it is excited only by the actuator (the shaker being still connected and short-circuited), is shown in

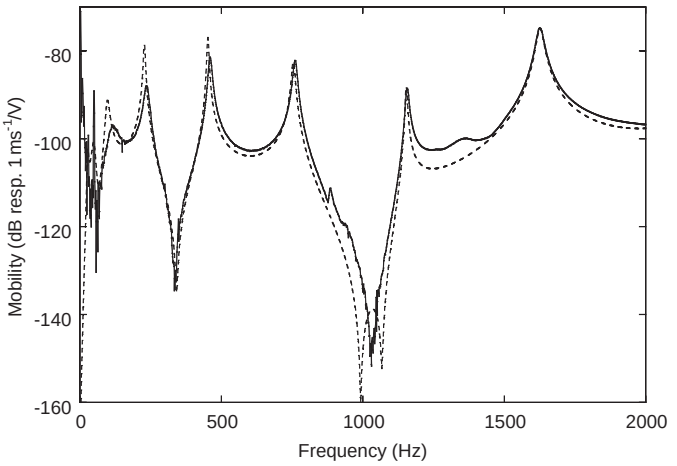

Fig. 10. Mobility of beam treated with ACL and excited with actuator only: ——, measured; - - -, calculated.

Fig. 10. In this case, the reference used to calculate the transfer function is the voltage sent to the actuator. In both cases, good agreement is reached between theoretical and experimental results. Therefore, the response of the closed-loop system can be accurately predicted, provided that the amplitudes and phases of the applied force and voltage are known.

4. Quantification of damping mechanisms

Quantifying the different damping mechanisms involved in ACL treatments is essential in order to optimise them. In this work, the efficiency of these mechanisms is quantified by a set of indices. Their definitions involve the kinetic energy, the total power input into the structure, and the power dissipated in the shearing of the viscoelastic layer and in the other dissipation mechanisms that might be present on the structure.

When a control voltage is applied to the actuator, the efficiency of the treatment will, hopefully, increase, resulting in a reduction of the vibrational energy in the structure. This reduction can be quantified by comparing the level of energy in the structure, with and without control. The kinetic energy is chosen since it characterises the vibrational level of the structure. Therefore an index R_{active}, in dB, is defined as

$$R_{\text{active}} = 10 \log \frac{E_{\text{kin,passive}}}{E_{\text{kin,active}}}, \tag{51}$$

where E_{kin} is the time-averaged kinetic energy of the structure, given by

$$E_{\text{kin}} = \frac{\rho L}{2} \omega^2 \int_0^L W_{\text{rms}}^2 \, \mathrm{d}x, \tag{52}$$

where the subscript rms refers to the root mean square value. This index quantifies the efficiency of the active control.

The reduction of kinetic energy quantified by R_{active} is due both to the increased efficiency of the energy dissipation mechanisms in the structure, and to the bending moments applied to the structure by the actuator. The first of these mechanisms can be quantified by comparing the efficiency of the dissipation mechanisms to dissipate kinetic energy, with or without control. This results in an index R_{lost} defined as

$$R_{\text{lost}} = 10 \log \frac{(P_{\text{lost}}/E_{\text{kin}})_{\text{active}}}{(P_{\text{lost}}/E_{\text{kin}})_{\text{passive}}}, \tag{53}$$

where P_{lost} is the power lost in the mechanisms of dissipation of energy. In the case of a beam suspended on springs like the one described in Section 2.4,

$$P_{\text{lost}} = P_{\text{shear}} + P_{\text{springs}}, \tag{54}$$

where P_{shear} is the power dissipated in the shearing of the viscoelastic layer, and P_{springs} is the power dissipated in the suspension springs. P_{shear} is given by

$$P_{\text{shear}} = \frac{bt_v}{2} \int_{L_1}^{L_2} \text{Re}\{\tau \dot{\gamma}^*\} \, \text{d}x, \tag{55}$$

where γ is the shear strain in the viscoelastic layer, given in Eq. (49), and $\tau = G\gamma$ is the shear stress. P_{springs} is given by

$$P_{\text{springs}} = \tfrac{1}{2} \text{Re}\{F_{K_1} \dot{w}^*(0)\} + \tfrac{1}{2} \text{Re}\{F_{K_2} \dot{w}^*(L)\}, \tag{56}$$

where F_{K_1} and F_{K_2} are the forces applied by the suspension springs at $x = 0$ and L, as defined in Eqs. (24) and (27).

The bending moments applied by the actuator to the structure can have two effects: they can absorb energy from the structure, or they can change the impedance of the structure and therefore the power input by other external forces. In both cases, the result is a change of the total power input P_{in} into the structure. Therefore, the increase of efficiency due to the bending moments can be quantified by comparing the total power input into the structure, with and without control. Accordingly an index R_{in} is defined as

$$R_{\text{in}} = 10 \log \frac{P_{\text{in,passive}}}{P_{\text{in,active}}}. \tag{57}$$

The power input P_{in} is the sum of the power input by the external forces, P_{ext}, given by

$$P_{\text{ext}} = \tfrac{1}{2} \text{Re}\{F \dot{W}^*(0)\}, \tag{58}$$

and of the power input by the actuator, P_a, given by

$$P_a = \int_{L_1}^{L_2} bt_c \tfrac{1}{2} \text{Re}\{\sigma_a(x) \dot{\varepsilon}^*(x)\} \, \text{d}x. \tag{59}$$

Note that P_a can be negative if the actuator is absorbing energy. In the expression above, σ_a is the stress in the actuator due to the voltage applied to the actuator: $\sigma_a = -E_c \varepsilon_p = -d_{31} V_c / t_c$. Assuming that the control voltage V_c is constant over the electrodes of the actuator, Eq. (59) can

be rewritten

$$P_a = \tfrac{1}{2} b t_c \,\mathrm{Re}\left\{ \sigma_a(x) \int_{L_1}^{L_2} \dot{\varepsilon}^*(x)\,\mathrm{d}x \right\} = \tfrac{1}{2} b t_c \,\mathrm{Re}\{\sigma_a[\dot{U}(L_2) - \dot{U}(L_1)]\}. \tag{60}$$

If the dissipation of energy in the base and cover layers is neglected, and under stationary conditions, the power input into the system P_{in} is equal to the dissipated power P_{lost}; accordingly,

$$R_{\mathrm{in}} + R_{\mathrm{lost}} = 10 \log \left(\frac{(P_{\mathrm{lost}}/E_{\mathrm{kin}})_{\mathrm{active}}}{(P_{\mathrm{lost}}/E_{\mathrm{kin}})_{\mathrm{passive}}} \frac{P_{\mathrm{lost,passive}}}{P_{\mathrm{lost,active}}} \right) = R_{\mathrm{active}}. \tag{61}$$

In other words, the increase of efficiency of the treatment due to the actuator is the sum of the efficiency resulting from the decrease of input power into the structure, and of the increased efficiency of the energy dissipation in the shearing of the viscoelastic layer.

To complete the picture, it is necessary to quantify also the efficiency of the treatment in passive configuration. This efficiency can be quantified simply by the conventional loss factor

$$\eta = \frac{P_{\mathrm{shear}}}{2\pi E_{\mathrm{rev}}},$$

where E_{rev} is the reversible energy of the system. Alternatively, an index R_{passive} can be defined as

$$R_{\mathrm{passive}} = 10 \log \left(\frac{E_{\mathrm{kin}}}{E_{\mathrm{kin}_0}} \right)_{\mathrm{passive}}, \tag{62}$$

where E_{kin_0} is the kinetic energy calculated with the loss factor of the viscoelastic layer set to zero. The kinetic energy E_{kin_0} depends on the loss factor of the base and cover beams. Nevertheless, the advantage of this index is that it is possible to compare it with the other indices, and to define the total efficiency of the ACL treatment simply as the sum of the passive efficiency and of the active efficiency:

$$R_{\mathrm{tot}} = 10 \log \left(\frac{E_{\mathrm{kin,passive}}}{E_{\mathrm{kin}_0,\mathrm{active}}} \right) = R_{\mathrm{passive}} + R_{\mathrm{active}}. \tag{63}$$

In other words, the overall efficiency of the treatment is the sum of its efficiency in the passive configuration, and of the efficiency added by the motion of the actuator.

5. Parameter study on a beam fully treated with ACL

To illustrate the approach proposed in the previous section, a parameter study is made on a beam fully treated with ACL. This study is investigating the repartition of the damping mechanisms, when the control voltage is chosen to maximise the efficiency of the active control. Results are obtained for different modes and different values of the shear modulus G of the viscoelastic layer.

For the sake of simplicity, the study is made on a freely suspended beam, so that the only mechanism of dissipation of energy is the shearing of the viscoelastic layer. The properties of the beam, the viscoelastic layer and the PZT actuator are the same as in the experimental study (see Tables 1–3 in Section 3), except for the shear modulus G, which is supposed to be independent of

frequency. The loss factor associated with G is fixed to 1, and the storage modulus is varied between 50 and 8000 kN/m^2.

The amplitude of the excitation force at the position $x = 0$ is fixed to 1 N. The amplitude and phase of the control voltages maximising the indices R_{in}, R_{lost} and R_{active} are obtained by using a numerical optimisation. The indices $R_{passive}$, R_{in}, R_{lost}, R_{active} and R_{total} are calculated for the selected values of the control voltage and for the different values of the shear modulus, in the frequency range up to 2.5 kHz. To reduce the amount of data and for easier interpretation, the results are integrated over each mode's range of frequency. As an example, the integration of R_{lost} for a given mode n is done as follows

$$R_{\mathrm{lost},n} = 10\log\frac{(\int_{f_{\min,n}}^{f_{\max,n}} P_{\mathrm{lost}}\,\mathrm{d}f / \int_{f_{\min,n}}^{f_{\max,n}} E_{\mathrm{kin}}\,\mathrm{d}f)_{\mathrm{active}}}{(\int_{f_{\min,n}}^{f_{\max,n}} P_{\mathrm{lost}}\,\mathrm{d}f / \int_{f_{\min,n}}^{f_{\max,n}} E_{\mathrm{kin}}\,\mathrm{d}f)_{\mathrm{passive}}}, \tag{64}$$

where $f_{\min,n}$ and $f_{\max,n}$ are the frequency limits associated with mode f. These limits are determined from the minima preceding and following the resonance of mode n, in the curve P_{ext} calculated for the open-loop configuration. The integration for the other indices are done similarly to Eq. (64).

In the case of a fully treated beam, the coverage of the actuator is symmetrical; thus only odd modes can be controlled. With the parameters chosen in this work, data for the first, third, fifth and seventh modes are obtained.

In Fig. 11, $R_{passive}$ and the optimised values of R_{active} and R_{total} are presented for the different values of G and the different modes. It shows that $R_{passive}$ reaches at least 15 dB, except for the first mode. This is an expected result, since in practice passive treatments with viscoelastic materials

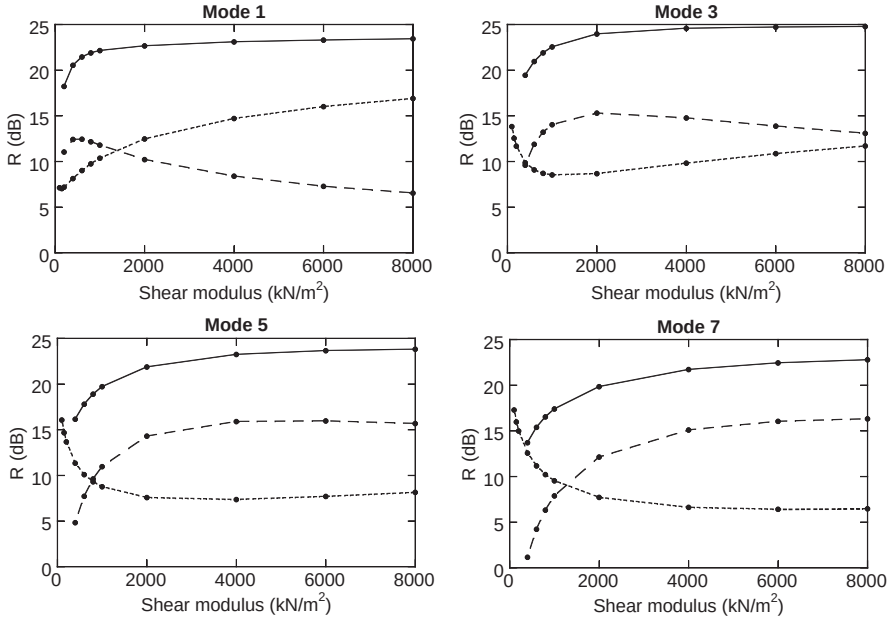

Fig. 11. Indices calculated with the control voltage optimising R_{active}: - - -, $R_{passive}$; · · · ·, R_{active}; ——, R_{total}.

are generally less efficient at low frequencies. Results also show that R_{active} is higher when $R_{passive}$ is low. This shows that the effects of active control and of material damping in ACL treatment complement each other, since the active control improves the treatment when the passive damping is the least efficient. When designing the treatment, this means that the parameters should be chosen so that the active control is efficient at low frequencies, where it is easier to implement it, and the attenuation of the high frequencies is left to the passive damping. With this purpose, it is better to choose a high value of the shear modulus of the viscoelastic layer. This approach is different to the one proposed by most authors, who first choose the material and geometric parameters of the treatment to optimise the passive damping characteristics first, and then design the control system to optimise the active damping. This could lead to a treatment with better fail-safe characteristics, but with suboptimal efficiency. Fig. 11 also indicates that a stiff viscoelastic layer leads to a high value of R_{active}, which is an additional argument for choosing a high shear modulus for the viscoelastic layer.

Fig. 12 shows the contribution of R_{in} and R_{lost} to R_{active}. Decreasing the shear modulus G has opposite effects on R_{in} and R_{lost}. R_{in} decreases for smaller G, which is logical since the forces transmitted to the host structure are smaller if the viscoelastic layer is soft, while R_{lost} increases. R_{in} can be negative, meaning that when the active control is optimised, the power input into the structure can be increased rather than decreased. The reason for this appears when looking at the amplitude and phase of the control voltages optimising the different active control mechanisms (see Figs. 13 and 14). The control voltages optimising R_{in} and R_{lost} are different from each other, especially for high modes and low values of the shear modulus. These figures also show that with the parameters considered in this study, the voltage optimising R_{active} is close to the one optimising R_{lost}. In other words, to actively control the kinetic energy of the beam, it is more

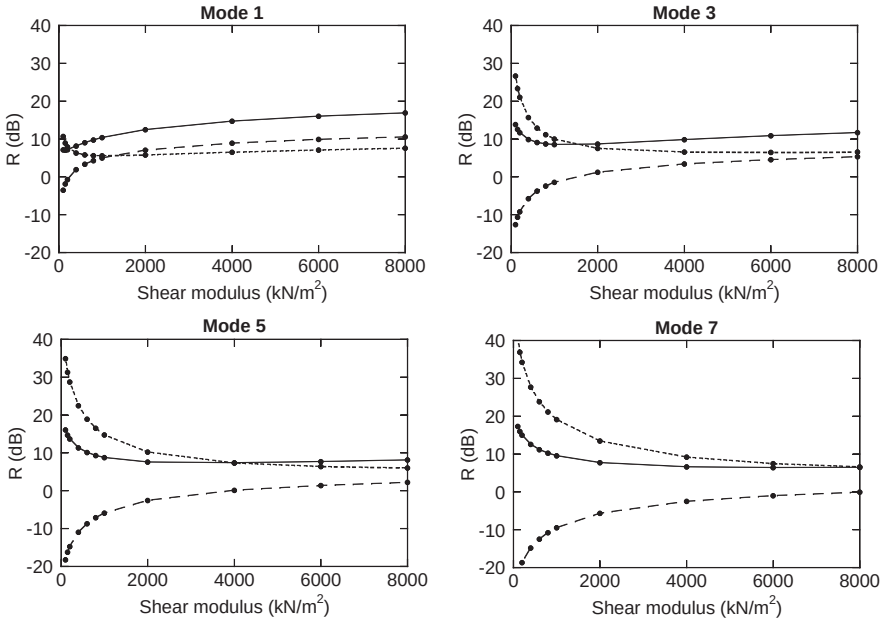

Fig. 12. Indices calculated with the control voltage optimising R_{active}: - - -, R_{in}; · · · · ·, R_{lost}; ——, R_{active}.

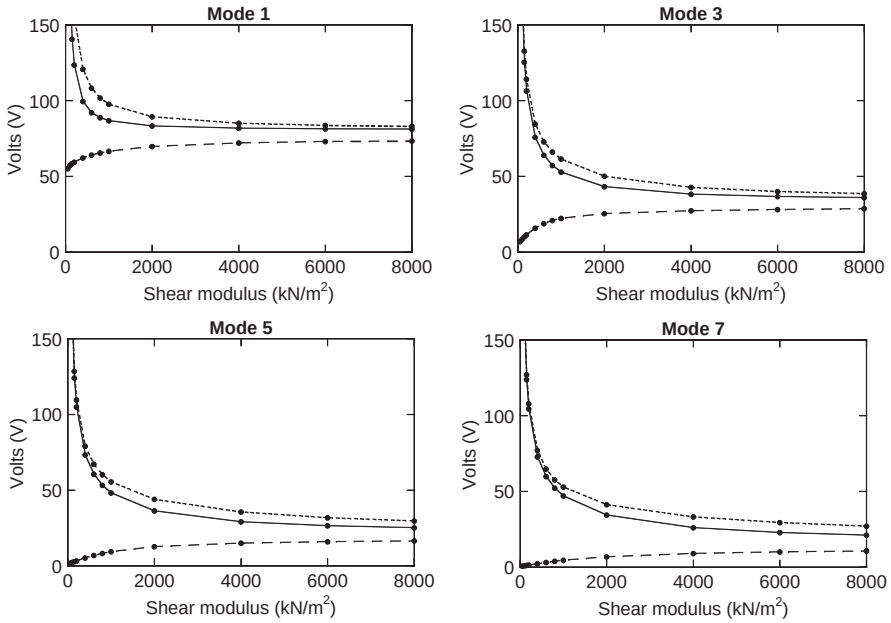

Fig. 13. Amplitude of the control voltages optimising the indices (excitation force: 1 N): - - -, R_{in}; · · · · ·, R_{lost}; ——, R_{active}.

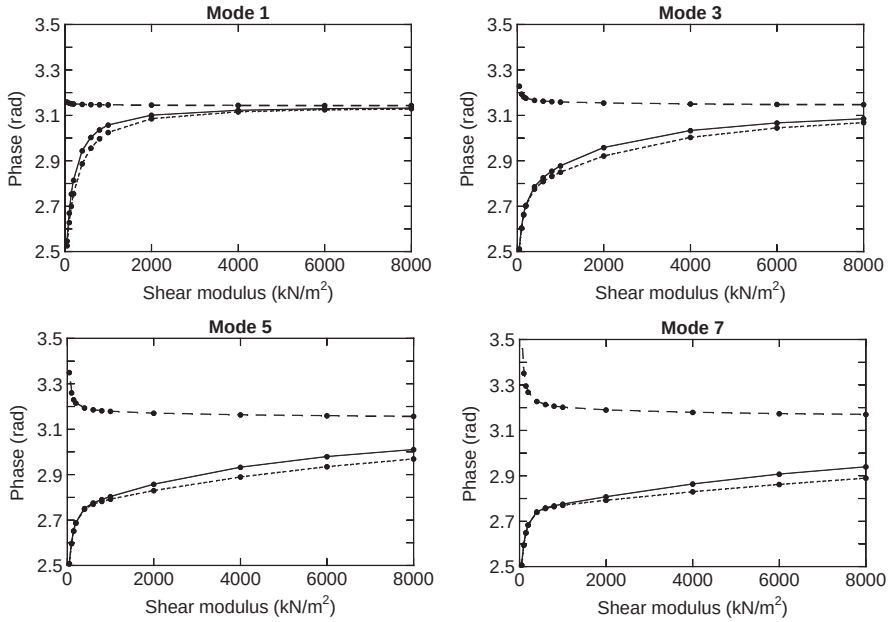

Fig. 14. Phase of the control voltages optimising the indices (excitation force: 1 N): - - -, R_{in}; · · · · ·, R_{lost}; ——, R_{active}.

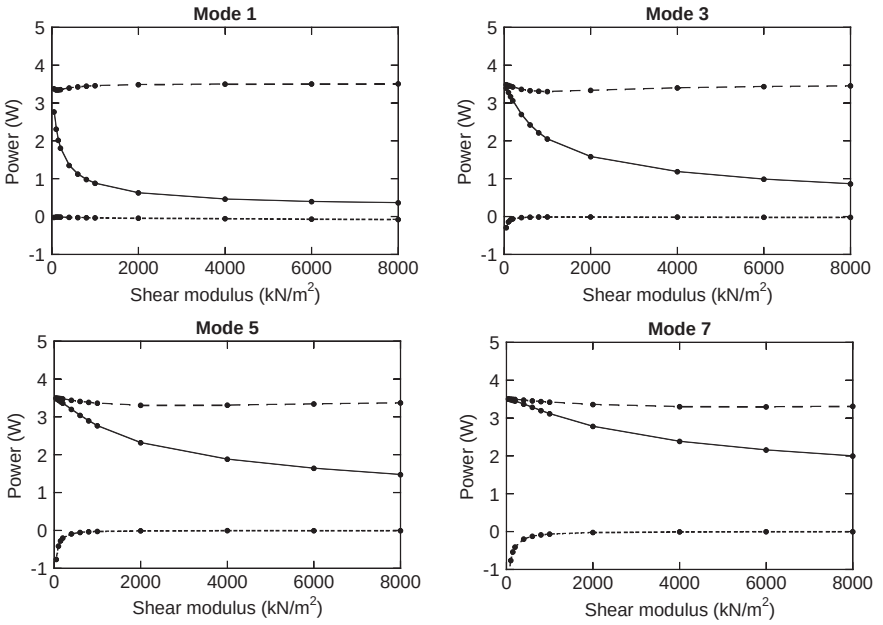

Fig. 15. Powers calculated with the control voltage optimising R_{in} (excitation force: 1 N): - - -, $P_{ext,passive}$; ——, $P_{ext,active}$; · · · · ·, P_a.

efficient in the present case to improve the material damping than to try to reduce the input power into the beam.

In addition, Figs. 13 and 14 indicate that if the value of the shear modulus is increased, the curves representing the amplitude and phase of the control voltage become flatter. This means that if a stiff viscoelastic layer is chosen, its shear modulus does not need to be accurately known to find the control voltage optimising the performance of the ACL treatment. Furthermore, this performance is less sensitive to changes of the shear modulus that might be caused by temperature variations.

It is interesting to get further insight into the reduction of the total input power P_{in} and to know if this reduction is due to an absorption of power by the actuator, or to a reduction of the power input by external sources of excitation. When the control voltage is selected to maximise R_{in} (i.e to minimise the total power input P_{in}), it appears that the actuator does not feed any power into the structure, and the power input from external sources is decreased (see Fig. 15). If instead the control voltage is chosen to maximise R_{active} (i.e. to minimise the kinetic energy in the structure), the power input from external sources is strongly reduced and is even close to zero for the first mode, and the actuator inputs power into the structure (see Fig. 16). This power input can be very small, in the case of the first mode, but becomes very large at high modes and for low values of the shear modulus. In both cases, optimising R_{in} or R_{active} does not lead to an absorption of power by the actuator. Thus, optimising the active control does not lead to a maximisation of the power absorbed by the actuator. This could indicate that the control law proposed by Baz [5] and by Shen [4], which ensures absorption of energy by the actuator, might guarantee the stability of the control but not its best performance.

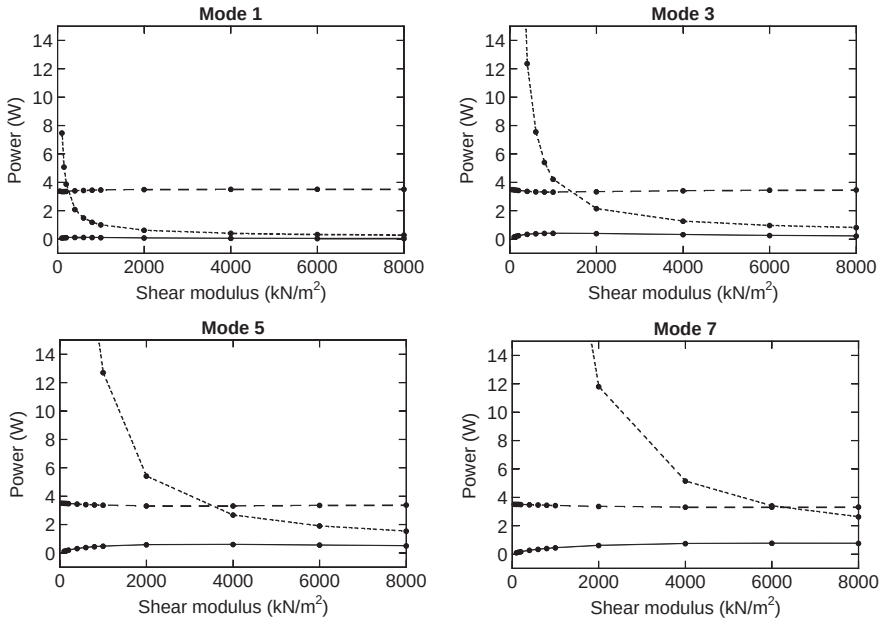

Fig. 16. Powers calculated with the control voltage optimising R_{active} (excitation force: 1 N): - - -, $P_{\text{ext,passive}}$; ——, $P_{\text{ext,active}}$; · · · · ·, P_a.

6. Numerical study on a beam partially treated with ACL

The indices presented in Section 4 are computed for a beam suspended on springs and partially treated with ACL. The characteristics of the beam, the suspension springs and the ACL treatment considered in this numerical study are the same as the ones used in the experiments described in Section 3.3. As a consequence, the ACL treatment covers only a small portion of the beam, the shear modulus of the viscoelastic layer varies with frequency and energy is dissipated at the boundaries of the beam. This allows the investigation of the damping mechanisms of ACL treatments in conditions approaching situations found in reality.

The ACL patch starts at 19.8 cm from the excited end of the beam and is 5 cm long, which corresponds to a position slightly off-centre of the beam. The complex stiffnesses of the spring, estimated from the experimental data presented in Section 3.3, are $K_1 = 2,9\,(1 + 0.28\text{i})$ kN/m and $K_2 = 2,5\,(1 + 0.31\text{i})$ kN/m.

The results are computed in the frequency range up to 2 kHz, and are integrated over each mode's range of frequency as described in Eq. (64). The amplitude of the excitation force at the position $x = 0$ is fixed to 1 N.

It is interesting to note that the resulting curves, given in Figs. 17–23, are not smooth as for R_{in} and R_{lost}, but their sum R_{active} is smooth, indicating that the unevenness cancels out. The reason for this phenomenon is yet unclear.

Fig. 17 shows that in the passive configuration, most of the damping at low frequencies is due to the dissipation of energy in the suspension springs. As a consequence, only little improvement is brought by the ACL treatment in passive configuration and limited improvement is brought by the actuator motion at these frequencies, as can be seen in Fig. 18. In the frequency range of the

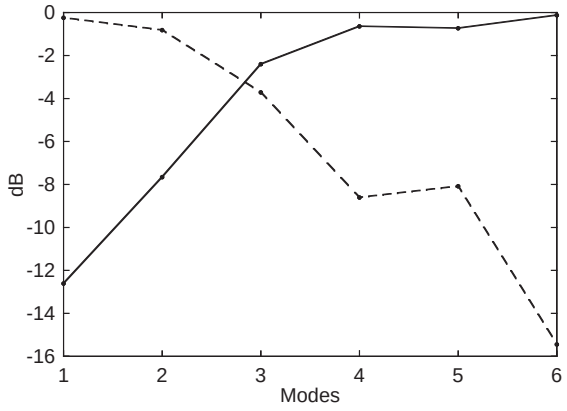

Fig. 17. P_{shear} and P_{springs} in the passive configuration: ——, $P_{\text{shear}}/P_{\text{lost}}$; - - -, $P_{\text{springs}}/P_{\text{lost}}$.

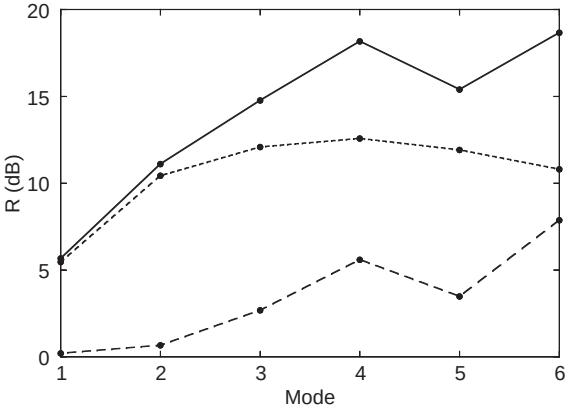

Fig. 18. Indices calculated with the control voltage optimising R_{active}: - - -, R_{passive}; · · · · ·, R_{active}; ——, R_{total}.

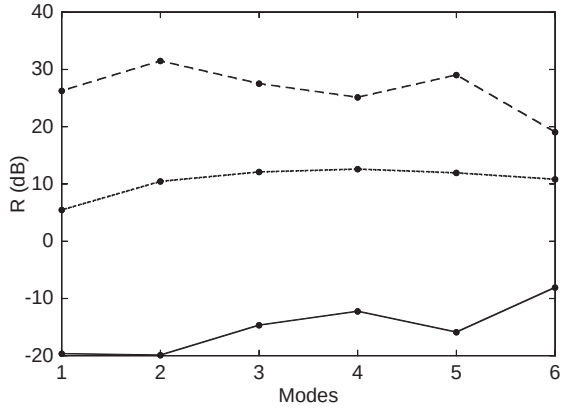

Fig. 19. Indices calculated with the control voltage optimising R_{active}: ——, R_{in}; - - -, R_{lost}; · · · · ·, R_{active}.

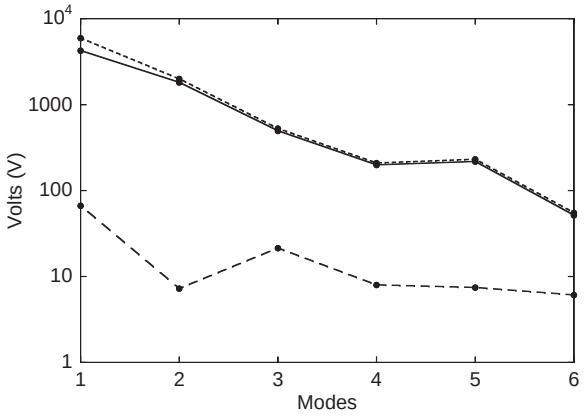

Fig. 20. Amplitude of the control voltages optimising the indices (excitation force: 1 N): - - -, R_{in}; · · · · ·, R_{lost}; ——, R_{active}.

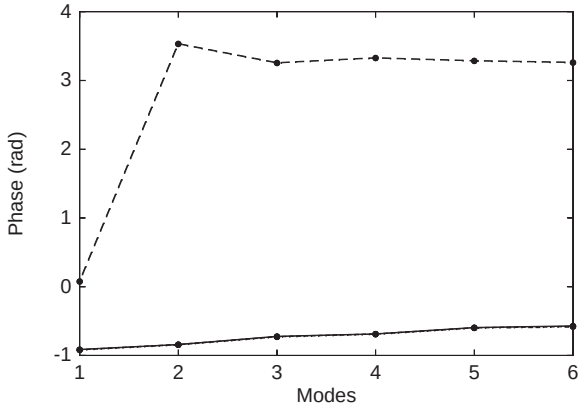

Fig. 21. Phase of the control voltages optimising the indices (excitation force: 1 N): - - -, R_{in}; · · · · ·, R_{lost}; ——, R_{active}.

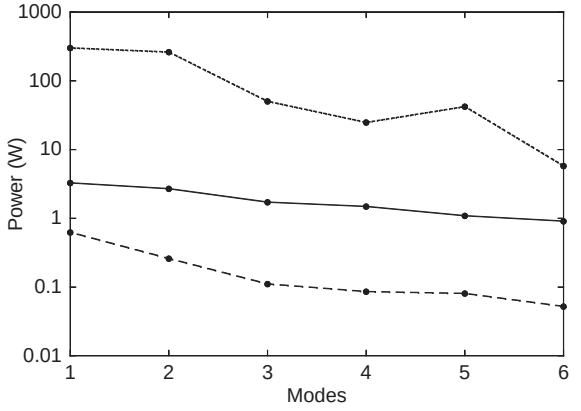

Fig. 22. Powers calculated with the control voltage optimising R_{active}: ——, $P_{ext,passive}$; - - -, $P_{ext,active}$; · · · · ·, P_a.

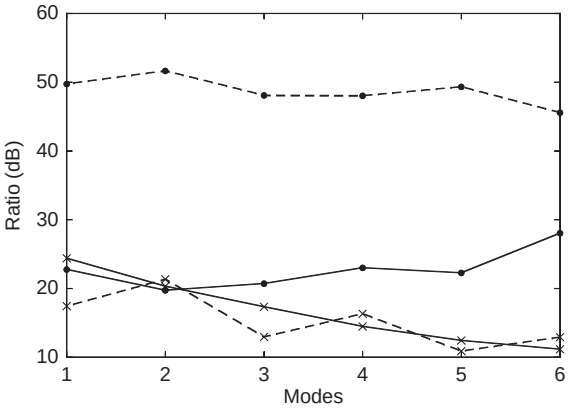

Fig. 23. Efficiency of the dissipation in the viscoelastic layer and in the suspension springs, with the control voltage optimising R_{active}: —●—, $P_{\text{shear}}/E_{\text{kin}}$ (passive case); - ● -, $P_{\text{shear}}/E_{\text{kin}}$ (active case); —×—, $P_{\text{springs}}/E_{\text{kin}}$ (passive case); - × -, $P_{\text{springs}}/E_{\text{kin}}$ (active case).

first bending resonances of the beam, the shear modulus G of the viscoelastic layer is less than $1000\,\text{kN/m}^2$. The results of the parameter study done in the previous section showed that this is a low value for the viscoelastic layer (see Figs. 11–16), and although the loss factor is highest in this frequency range, the active action of the ACL treatment has little effect and the optimum control voltage is very high (Fig. 20). This phenomenon might be stressed by the size of the actuator which is small relative to the wavelength of the bending motion at low frequencies, and which makes it difficult to control the beam at these frequencies.

Most of the improvement brought by the action of the actuator is due to augmented efficiency of the shearing in the viscoelastic layer, as can be seen in Fig. 19. As a consequence, when the control voltage is chosen to maximise R_{active}, the actuator inputs a large amount of power into the beam and R_{in} is negative. The effect of the actuator action on the efficiency of the dissipation of energy in the suspension springs is negligible, as shown in Fig. 23.

7. Conclusion

A model of a beam partially or fully treated with ACL was presented. It is based on the wave approach and is a modified version of Baz' model [13,14]. The model was experimentally validated and excellent agreement was reached up to 2 kHz. No control law is included in the model, so that the control voltage sent to the actuator can be chosen to be any value, and its effect on the damping mechanisms can be studied.

An approach to quantify separately the efficiency of the damping mechanisms of ACL treatments was proposed. A series of indices, based on the kinetic energy of the structure and on the power flows in and out of the structure, were defined. The index quantifying the total efficiency of the treatment is the sum of two other indices, one quantifying the efficiency of the treatment in open-loop, and the other, the efficiency added by the motion of the actuator. This latter is the sum of two indices. One quantifies the reduction of input power into the structure due to the active control; the other quantifies the increase of efficiency of the dissipation of energy in

the shearing of the viscoelastic layer or in other damping mechanisms in the structure, e.g. at the boundaries.

This approach is illustrated with a parameter study done on a freely suspended beam, fully treated with ACL. In this study, the shear modulus of the viscoelastic layer, assumed to be constant over frequency, is varied. Although this parameter study is not comprehensive, interesting conclusions can be drawn from the results. It shows that the passive and active components of ACL complement each other, since the active control can compensate a low efficiency of the passive control. This suggests that it is desirable to design the treatment so that the material damping focuses on a given frequency range while the active control is in charge of the remaining frequencies. Also, the effect of the absorption of power is small or null when the efficiency of the active control, or of the reduction of input power, are optimised. This indicates that the control law proposed by Baz [5] and by Shen [4], which ensures absorption of energy by the actuator, might guarantee the stability of the control but not its best performance.

The study also suggests that a high shear modulus of the viscoelastic layer seems preferable for several reasons. A stiff viscoelastic layer leads to a high overall efficiency of the ACL treatment; in the same time, the performance of the active actions is less sensitive to uncertainties of the shear modulus, and thus to temperature variations; lastly, choosing a stiff viscoelastic layer allows the application of the passive damping to the highest frequencies in the range of interest; this way, the active control is directed to the lower frequencies, where it is easier to implement.

The indices are also computed for a beam partially treated with ACL, and suspended on soft springs at its two ends. The results of this study demonstrate that with the chosen parameters, the viscoelastic layer is very soft at low frequencies (or high temperature) and the efficiency of the ACL treatment is limited. This suggests that separating the passive and active components of the ACL treatment, by bonding the actuator directly to the beam and using a passive constrained layer as proposed by Lam et al. [16] might be a better solution, because in this case the action of the actuator does not depend on the temperature and frequency dependence of the viscoelastic layer. On the other hand, the studies in this work showed that most of the improvement brought by the action of the actuator is due to an increased efficiency of the dissipation of energy in the viscoelastic layer; this effect would not occur if the actuator is bonded directly to the beam. This is still a matter of discussion, that the approach proposed in this work might help to clarify.

The two studies demonstrate the usefulness of the indices proposed in this work for allowing insight into the damping mechanisms of ACL treatments. More work is needed to compare the conventional ACL configuration to the one proposed by Lam, to design a control strategy and to optimise the parameters of ACL treatments.

Acknowledgements

This research is supported by a grant from Volvo Research Foundation, Volvo Educational Foundation, Dr. Pehr Gyllenhammar Research Foundation, and the Swedish Research Council.

Appendix

$$
\mathbf{A} = \begin{bmatrix}
(k^3+p_1)\mathrm{e}^{-kL_1} & -k^3+p_1 & -\mathrm{j}k^3+p_1 & \mathrm{j}k^3+p_1 & 0 & 0 & 0 & 0 \\
k^2\mathrm{e}^{-kL_1} & k^2 & -k^2 & -k^2 & 0 & 0 & 0 & 0 \\
0 & 0 & 0 & 0 & 0 & 0 & 0 & 0 \\
0 & 0 & 0 & 0 & 0 & 0 & 0 & 0 \\
1 & \mathrm{e}^{-kL_1} & \mathrm{e}^{\mathrm{j}kL_1} & \mathrm{e}^{-\mathrm{j}kL_1} & -\mathrm{e}^{-\delta_1\Delta L} & -\mathrm{e}^{-\delta_1 L_1} & -\mathrm{e}^{-\delta_2\Delta L} & -\mathrm{e}^{-\delta_2 L_1} \\
k & -k\mathrm{e}^{-kL_1} & \mathrm{j}k\mathrm{e}^{\mathrm{j}kL} & -\mathrm{j}k\mathrm{e}^{-\mathrm{j}kL} & -\delta_1\mathrm{e}^{-\delta_1\Delta L} & \delta_1\mathrm{e}^{-\delta_1 L_1} & -\delta_2\mathrm{e}^{-\delta_2\Delta L} & \delta_2\mathrm{e}^{-\delta_2 L_1} \\
B_bk^2 & B_bk^2\mathrm{e}^{-kL_1} & -B_bk^2\mathrm{e}^{\mathrm{j}kL} & -B_bk^2\mathrm{e}^{-\mathrm{j}kL} & R_1\mathrm{e}^{-\delta_1\Delta L} & R_1\mathrm{e}^{-\delta_1 L_1} & R_2\mathrm{e}^{-\delta_2\Delta L} & R_2\mathrm{e}^{-\delta_2 L_1} \\
-B_bk^3 & B_bk^3\mathrm{e}^{-kL_1} & B_bk^3\mathrm{e}^{\mathrm{j}kL} & -B_bk^3\mathrm{e}^{-\mathrm{j}kL} & -P_1\mathrm{e}^{-\delta_1\Delta L} & P_1\mathrm{e}^{-\delta_1 L_1} & -P_2\mathrm{e}^{-\delta_2\Delta L} & P_2\mathrm{e}^{-\delta_2 L_1} \\
0 & 0 & 0 & 0 & Q_1\mathrm{e}^{-\delta_1\Delta L} & Q_1\mathrm{e}^{-\delta_1 L_1} & Q_2\mathrm{e}^{-\delta_2\Delta L} & Q_2\mathrm{e}^{-\delta_2 L_1} \\
0 & 0 & 0 & 0 & -1 & -\mathrm{e}^{-\delta_1 L_2} & -1 & -\mathrm{e}^{-\delta_2 L_2} \\
0 & 0 & 0 & 0 & -\delta_1 & \delta_1\mathrm{e}^{-\delta_1 L_2} & -\delta_2 & \delta_2\mathrm{e}^{-\delta_2 L_2} \\
0 & 0 & 0 & 0 & R_1 & R_1\mathrm{e}^{-\delta_1 L_2} & R_2 & R_2\mathrm{e}^{-\delta_2 L_2} \\
0 & 0 & 0 & 0 & -P_1 & P_1\mathrm{e}^{-\delta_1 L_2} & -P_2 & P_2\mathrm{e}^{-\delta_2 L_2} \\
0 & 0 & 0 & 0 & Q_1 & Q_1\mathrm{e}^{-\delta_1 L_2} & Q_2 & Q_2\mathrm{e}^{-\delta_2 L_2}
\end{bmatrix}
$$

$$
\begin{bmatrix}
0 & 0 & 0 & 0 & 0 & 0 \\
0 & 0 & 0 & 0 & 0 & 0 \\
0 & 0 & k^3-p_2 & (-k^3-p_2)\mathrm{e}^{-kL} & (-\mathrm{j}k^3-p_2)\mathrm{e}^{\mathrm{j}kL} & (\mathrm{j}k^3-p_2)\mathrm{e}^{-\mathrm{j}kL} \\
0 & 0 & k^2 & k^2\mathrm{e}^{-kL} & -k^2\mathrm{e}^{\mathrm{j}kL} & -k^2\mathrm{e}^{-\mathrm{j}kL} \\
-\mathrm{e}^{-\delta_3\Delta L} & -\mathrm{e}^{-\delta_3 L_1} & 0 & 0 & 0 & 0 \\
-\delta_3\mathrm{e}^{-\delta_3\Delta L} & \delta_3\mathrm{e}^{-\delta_3 L_1} & 0 & 0 & 0 & 0 \\
R_3\mathrm{e}^{-\delta_3\Delta L} & R_3\mathrm{e}^{-\delta_3 L_1} & 0 & 0 & 0 & 0 \\
-P_3\mathrm{e}^{-\delta_3\Delta L} & P_3\mathrm{e}^{-\delta_3 L_1} & 0 & 0 & 0 & 0 \\
Q_3\mathrm{e}^{-\delta_3\Delta L} & Q_3\mathrm{e}^{-\delta_3 L_1} & 0 & 0 & 0 & 0 \\
-1 & -\mathrm{e}^{-\delta_3 L_2} & \mathrm{e}^{-k(L-L_2)} & \mathrm{e}^{-kL_2} & \mathrm{e}^{\mathrm{j}kL_2} & \mathrm{e}^{-\mathrm{j}kL_2} \\
-\delta_3 & \delta_3\mathrm{e}^{-\delta_3 L_2} & k\mathrm{e}^{-k(L-L_2)} & -k\mathrm{e}^{-kL_2} & \mathrm{j}k\mathrm{e}^{\mathrm{j}kL_2} & -\mathrm{j}k\mathrm{e}^{-\mathrm{j}kL_2} \\
R_3 & R_3\mathrm{e}^{-\delta_3 L_2} & B_bk^2\mathrm{e}^{-k(L-L_2)} & B_bk^2\mathrm{e}^{-kL_2} & -B_bk^2\mathrm{e}^{\mathrm{j}kL_2} & -B_bk^2\mathrm{e}^{-\mathrm{j}kL_2} \\
-P_3 & P_3\mathrm{e}^{-\delta_3 L_2} & -B_bk^3\mathrm{e}^{-k(L-L_2)} & B_bk^3\mathrm{e}^{-kL_2} & \mathrm{j}B_bk^3\mathrm{e}^{\mathrm{j}kL_2} & -\mathrm{j}B_bk^3\mathrm{e}^{-\mathrm{j}kL_2} \\
Q_3 & Q_3\mathrm{e}^{-\delta_3 L_2} & 0 & 0 & 0 & 0
\end{bmatrix}
$$

$$\mathbf{F} = \left[F_{\text{ext}} \;\; 0 \;\; 0 \;\; 0 \;\; 0 \;\; 0 \;\; \frac{\mathrm{d}_{31} b \, \mathrm{d} E_b t_b E_c}{E_b t_b + E_c t_c} V_c \;\; 0 \;\; -\frac{\mathrm{d}_{31} b E_b t_b E_c}{E_b t_b + E_c t_c} V_c \;\; 0 \right.$$
$$\left. 0 \;\; \frac{\mathrm{d}_{31} b \, \mathrm{d} E_b t_b E_c}{E_b t_b + E_c t_c} V_c \;\; 0 \;\; -\frac{d_{31} b E_b t_b E_c}{E_b t_b + E_c t_c} V_c \right].$$

References

[1] W.H. Liao, K.W. Wang, On the analysis of viscoelastic materials for active constrained layer damping treatments, *Journal of Sound and Vibration* 207 (3) (1997) 319–334.

[2] D. Golla, P. Hughes, Dynamics of viscoelastic structures—a time-domain, finite element formulation, *Journal of Applied Mechanics* 52 (4) (1985) 897–906.

[3] D. McTavish, P. Hughes, Modeling of linear viscoelastic space structures, *Journal of Vibration and Acoustics* 115 (1) (1993) 103–110.

[4] I.Y. Shen, A variational formulation, a work-energy relation and damping mechanisms of active constrained layer treatments, *Journal of Vibration and Acoustics* 119 (2) (1997) 192–199.

[5] A. Baz, Boundary control of beams using active constrained layer damping, *Journal of Vibration and Acoustics* 119 (2) (1997) 166–172.

[6] A. Baz, Optimization of energy dissipation characteristics of active constrained layer damping, *Smart Materials and Structures* 6 (3) (1997) 360–368.

[7] F. Gandhi, B.E. Munsky, Comparison of the mechanism and effectiveness of position and velocity feedback in active constrained-layer damping treatments, in: *Proceedings of the SPIE The International Society for Optical Engineering*, Vol. 3989, 2000, pp. 61–72.

[8] W.H. Liao, K.W. Wang, Characteristics of enhanced active constrained layer damping treatments with edge elements, *Journal of Vibration and Acoustics* 120 (4) (1998) 886–893.

[9] Y. Liu, K. Wang, Active–passive hybrid constrained layer for structural damping augmentation, *Journal of Vibration and Acoustics* 122 (3) (2000) 254–262.

[10] M.C. Ray, A. Baz, Optimization of energy dissipation of active constrained layer damping treatments of plates, *Journal of Sound and Vibration* 208 (3) (1997) 391–406.

[11] C.R. Fuller, S. Elliott, P. Nelson, *Active Control of Vibration*, Academic Press, London, 1996.

[12] M.J. Brennan, S.J. Elliott, R.J. Pinnington, Strategies for the active control of flexural vibrations on a beam, *Journal of Sound and Vibration* 186 (4) (1995) 657–688.

[13] A. Baz, Active constrained layer damping, in: *Damping'93 Conference*, Vol. 3, San Francisco, CA, 1993, pp. IBB 1–23.

[14] A. Baz, J. Ro, Partial treatment of flexible beams with active constrained layer damping, in: *Conference of Engineering Science Society*, Vol. ASME-AMD 67, Charlottesville, VA, 1993, pp. 61–80.

[15] E.E. Ungar, Loss factors of viscoelastically damped beam structures, *Journal of the Acoustical Society of America* 34 (8) (1962) 1082–1089.

[16] M.J. Lam, D.J. Inman, W.R. Saunders, Vibration control through passive constrained layer damping and active control, *Journal of Intelligent Material Systems and Structures* 8 (8) (1997) 663–677.